Applied Surface Science 258 (2012) 3841–3845

Contents lists available at SciVerse ScienceDirect

Applied Surface Science

journal homepage: www.elsevier.com/locate/apsusc

Nanoporous structures of polyimide induced by Ar ion beam irradiation

Sk. Faruque Ahmed [a,*], Kwang-Ryeol Lee [a], Ju-il Yoon [b], Myoung-Woon Moon [a,**]

[a] Interdisciplinary and Fusion Technology Division, Korea Institute of Science and Technology, 136-791, Seoul, Republic of Korea
[b] Mechanical System Engineering, Hansung University, 136-792, Seoul, Republic of Korea

ARTICLE INFO

Article history:
Received 10 January 2011
Received in revised form 6 December 2011
Accepted 10 December 2011
Available online 19 December 2011

Keywords:
Ar ion beam
Polyimide
3D porous nanostructure
Hardness

ABSTRACT

The surface morphology evolution of polyimide (PI) that was treated with an Ar ion beam was explored using a hybrid ion beam system. A hole-like nanostructure formed on PI during the Ar ion beam treatment at a lower fluence, but PI formed 3D porous nanostructures with a mean diameter of ~90 nm at a higher fluence. The chemical binding energy and the composition of the Ar ion irradiated PI were analyzed using FT-IR and XPS spectra, which revealed that the polymer chain scissioning increased with increasing Ar ion treatment duration, i.e., fluence. The surface hardness and the elastic modulus of PI increased from 1.17 to 1.62 GPa and 4.06 to 5.41 GPa, respectively, with respect to the Ar ion beam treatment duration.

1. Introduction

Polyimide (PI) is a well known polymer with unique properties (e.g. recyclable, light weight, flexible, good thermal stability, and heat and chemical resistance) as well as excellent biocompatibility properties. Thus, PI has become a very common polymer in the semiconductor industry, electronics, sensors, the car industry, as well as in biomedical applications [1–3]. However, its surface properties are not adequate in terms of wettability, electrical conductivity, gas transmission, mechanical properties, such as hardness and elasticity, or adhesion for the above mentioned applications. For these reasons, a variety of surface modification techniques, such as chemical etching, plasmas, corona discharge, ion beam and others techniques, have been adopted in order to improve the various properties of PI [4–8]. Previous reports have shown that the surface treatment of PI with different ion beam/plasma irradiation affects the structural, mechanical, optical, electrical, and chemical properties of PI [2,3,6–11]. Kucheyev et al. reported that the hardness and the elastic modulus increase while the tensile strength decreased for PI that is irradiated with MeV ions (H, He and C). These properties linearly depended on the ion fluence and superlinearly depended on the electronic energy loss [10]. Additionally, during the O_2 or 100 keV N^+ ion beam irradiation of PI, the surface roughness and the peel strength increased more, while the contact angle decreased with respect to the ion dose [8,11].

However, no reports have examined the effects of a low energy (~keV) Ar ion beam on the 3D porous surface morphological evolution of PI in detail. In this work, it was reported that a low energy broad Ar ion beam treatment created peculiar 3D porous nanostructures on the PI surface. Any changes in the chemical bonds that were caused by the Ar ion beam treatment were explored using chemical analysis, which revealed that the chain scissioning increased in PI with increasing Ar ion beam treatment duration. The mechanical properties, including the hardness and the elastic modulus, were measured using Nano-indentation, and the coefficient of friction (COF) was determined for the PI surfaces that were covered by the nanostructure using a tribo-experiment. The improved mechanical properties were explained in terms of the surface morphology as well as the chemical composition changes that were induced by the Ar ion beam treatment.

2. Experimental details

The Ar ion beam treatment of PI was carried out in a hybrid ion beam system. The sample coupons with dimensions of 10 mm × 10 mm × 20 μm were placed in the ion beam chamber, and the chamber was evacuated to a base pressure of 2×10^{-5} mbar. The distance between the ion source and the substrate holder was approximately 15 cm. Ar gas was introduced into the end-Hall type ion gun at a flow rate of 8 sccm, and the anode voltage was kept constant at 1 keV with a current density of 50 μA/cm^2. A radio frequency (r.f.) bias voltage was applied to the substrate holder at −600 V with a corresponding current of 44 mA. The Ar ion beam

* Corresponding author. Present address: Department of Physics, Aliah University, DN-41, Sector-V, Salt Lake, Kolkata 700 091, India.
** Corresponding author.
E-mail addresses: faruquekist@gmail.com (Sk. Faruque Ahmed), mwmoon@kist.re.kr (M.-W. Moon).

0169-4332/$ – see front matter © 2011 Elsevier B.V. All rights reserved.
doi:10.1016/j.apsusc.2011.12.042

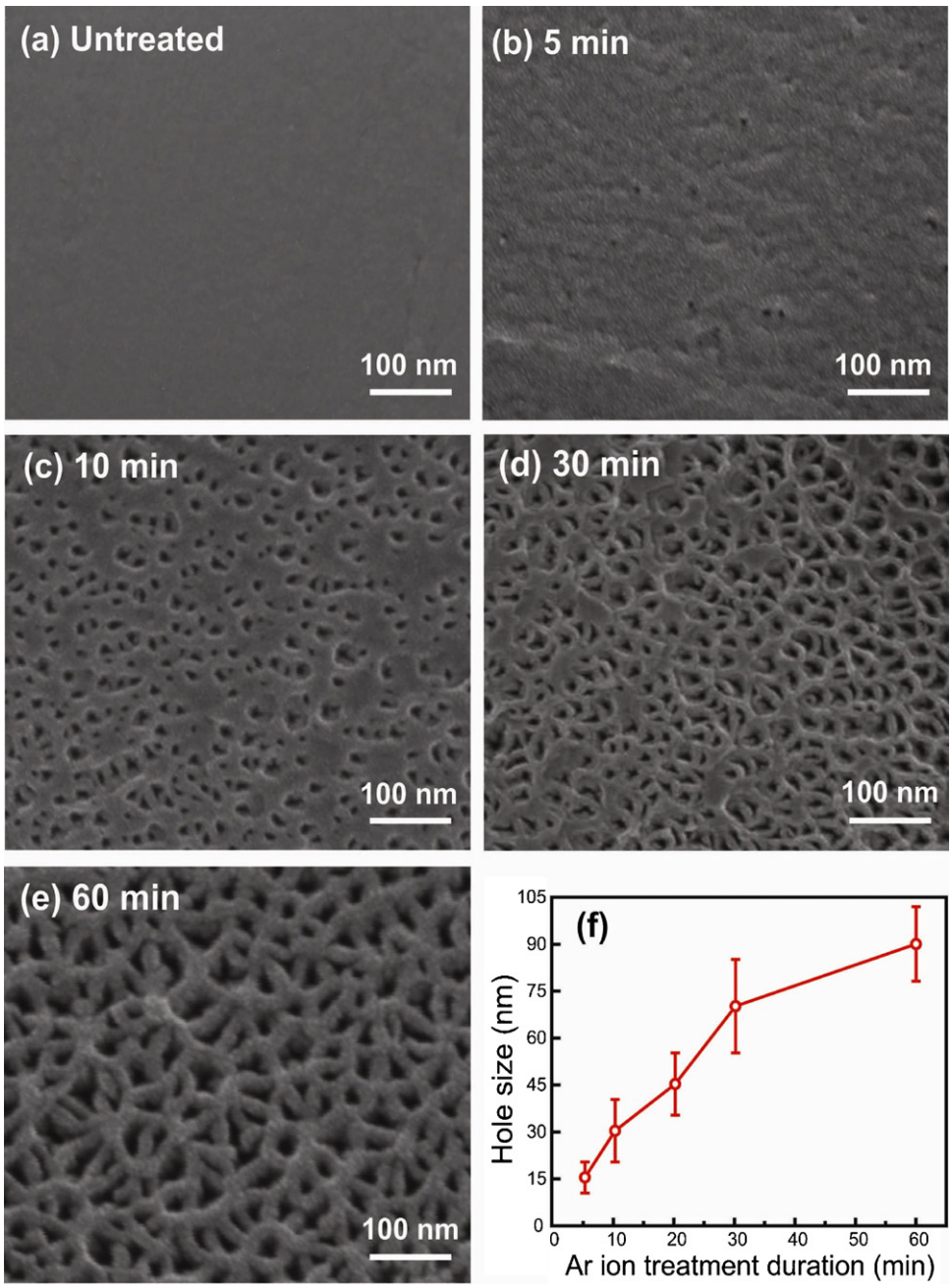

Fig. 1. SEM images of the untreated and Ar ion beam treated PI surfaces with (a–e) different treatment durations and (f) variations in the hole size for the Ar ion beam treatment.

exposure time varied from 5 to 60 min, corresponding to an ion fluence ranging from 9.6×10^{16} to 11.5×10^{17}, respectively. The eaching thickness or depth of the PI treated by Ar ion beam was measured about 3.38 nm/min using an atomic force microscope (AFM, Parksystem).

The surface morphology of the Ar ion beam treated PI was studied using a scanning electron microscope (SEM, NanoSEM, FEI Company). The Ar ion induced chemical change in PI was analyzed using Fourier transform infrared spectroscopy (FT-IR, Infinity Gold FT-IR, Thermo Mattson) and X-ray photoelectron spectroscopy (XPS, PHI 5800 ESCA system, Physical Electronics). A nanomechanical testing instrument (Triboindentor, Hysitron Inc.) with a Berkovich diamond tip (approximate radius of curvature of 150 nm) was used to measure the mechanical properties of the Ar ion beam treated PI surfaces. The single indentation mode was adopted in order to estimate the average values of the hardness and the elastic modulus for each of the samples up to a maximum load of 250 μN. The friction behavior of the PI sample was measured against a glass ball with a diameter of 6 mm using a custom-made device. The sliding distance was set to 1 mm at a constant speed of 10 μm/s. The measured frictional force in the steady sliding regime was divided by the normal force to estimate the average coefficient of friction.

3. Results and discussion

3.1. Surface morphology studies

The SEM images of the top view of the PI samples that were treated using the Ar ion beam are shown for different treatment durations in Fig. 1. The pristine PI substrate did not exhibit a specific

surface pattern (Fig. 1(a)), while a certain hole structure started to form after Ar ion beam treatment for 5 min. After Ar ion beam treatment for 10 min, holes formed with an average diameter of 25 nm (Fig. 1(c)). These types of nanoscale holes are generally observed for the chemically treatment of the heavy ion tracks of polyimide, in filter or membrane applications [12]. Fig. 1(d) shows the 3D nanostructure that formed over the PI surface after the 30 min treatment, whereas 3D porous nanostructures formed after irradiation for 60 min in Fig. 1(e). The diameter of the holes increased with increasing Ar ion treatment duration in Fig. 1(f). The Ar ion beam with a high colliding energy roughened the PI surface primarily through a physical ion bombardment because of the high atomic weight of the inert gas [8]. Also, the Ar ion treatment promoted the etching process and the impact of the active species that was generated in the Ar plasma, which increased the roughness as the ion beam treatment duration increased.

The morphology changed with increasing Ar ion treatment duration, even though the energy of the incident Ar ions was fixed at 1 keV for the anode voltage of the ion gun. The morphology that was induced by the ion/plasma irradiation was not only due to the ion species of the plasma but also depended on the total deposited energy of all of the species that were contained in the ion/plasma and the rate of the energy deposition as well as the ion beam incident angle [9,13]. During the ion irradiation on the polymer, the radiation affected the entire range of the ion track, producing a high yield, and the bond breakage of the organic molecules resulted in the formation of an ensemble of smaller molecules, many of which may be volatile [14,15]. The displacement of the target atoms by the energetic collisions can cause permanent damage to a polymer mainly in the form of chain scissioning through the displacement of the atoms from the polymer chains, creating various patterns of dots, steps, nano-pores, emboss-like nanostructures, nanofibers, and one-dimensional straight wrinkles to highly complex hierarchical undulations [9,13,16–18]. In Fig. 1, the hole and 3D porous nanostructure patterns that formed on PI were induced by the polymer etching, and the chain scissioning and fragmentation mechanism was confirmed using the FT-IR and XPS analysis in Figs. 2 and 3.

3.2. Fourier transformed infrared spectra analysis

The FT-IR spectra of the Ar ion beam treated PI samples were analyzed at different treatment durations in Fig. 2(a). The peaks at 835 cm^{-1} and 890 cm^{-1} were assigned to the C—H deformation. The peak at 3080 cm^{-1} was assigned to the C—H stretching, and the medium peak at 1470 cm^{-1} was assigned to the C—H bending modes [19]. The different weak, medium and strong peaks in the regions of 1050–1250 cm^{-1} and 1223–1290 cm^{-1} corresponded to the C—O and C—O—C stretching bonds, respectively. The strong peaks that were observed at 1520 and 3486 cm^{-1} were due to the N—H stretching, and the peaks at 1620 cm^{-1} and 1780 cm^{-1} were caused by the C=O asymmetric bond. The peak at 3625 cm^{-1} was attributed to the O—H bond. The broad prominent bands were observed because of the imide stretching and the cyclic imide groups near 1120 cm^{-1} and 1385 cm^{-1}, respectively, which were characteristics of PI [20].

Almost all of the above-mentioned bonds were gradually scissioned after the Ar ion beam treatment, which was confirmed by the decrease in the intensities of almost all of the peaks. The relative absorbance I/I_0 (where I_0 and I are the absorbance of the untreated and Ar ion beam treated PI samples, respectively) of some of the characteristic bonds was plotted against the Ar ion treatment duration in Fig. 2(b). It can be seen that, although the relative absorbance of all of the characteristic bonds decreased, the C—H and O—H bonds were scissioned at almost the same rate, whereas the scissioning of C—H at 890 cm^{-1} and the N—H bonds was comparatively rigorous.

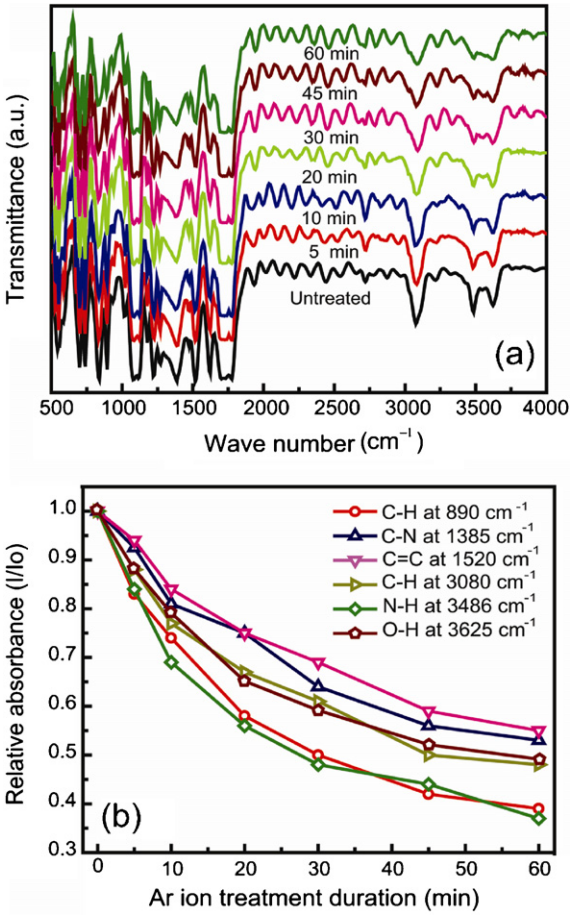

Fig. 2. (a) FT-IR spectra of the untreated and Ar ion beam treated PI and (b) changes of in the relative absorbance (I/I_0) for different bonds with respect to the Ar ion beam treatment duration.

On the other hand, the imide group and the C=C bonds, although scissioned, were relatively stable compared to the N—H and C—H bonds.

3.3. XPS analysis

The details of the chemical bonding states of carbon, oxygen, and nitrogen were also studied by analyzing the core-level XPS spectra of the elements. Fig. 3(a) shows that the oxygen atomic fraction increased from 13.1 to 21.4% as the Ar ion treatment duration increased from 0 to 60 min, while the carbon and nitrogen contents decreased from 80.6 to 75.8% and 6.3 to 2.9%, respectively. In particular, the decrease in the nitrogen amount was significant with increasing Ar ion treatment duration because of the selective sputtering of oxygen and nitrogen by the Ar ion beam and the resulting change in the different functional bonds, such as carbonyl (C=O), imide (C—N), and carboxyl (C—O) [8,19]. In the XPS full spectra of untreated PI (not shown here), the C1s peaks at approximately 286.4 eV for the untreated polyimide, N1s peaks at approximately 402.4 eV, and O1s peaks at approximately 532.5 eV are observed. The C1s XPS spectra here were shifted to a lower binding energy by approximately 1.8 eV due to an electron charging effect. Ektessabi and Hakamata also observed the similar type shifting of peak position due to charging effect of Ar, O_2 and N_2 irradiated PI films [20]. The C1s core level XPS spectra of the untreated and the Ar ion beam treated PI were deconvoluted into four peaks having binding energies of 284.6, 285.6, 286.4, and 288.5 eV for the C—C/C—H, C—N, C—O, and C=O bonds, respectively, in Fig. 3(b) [11]. Fig. 3(c) shows

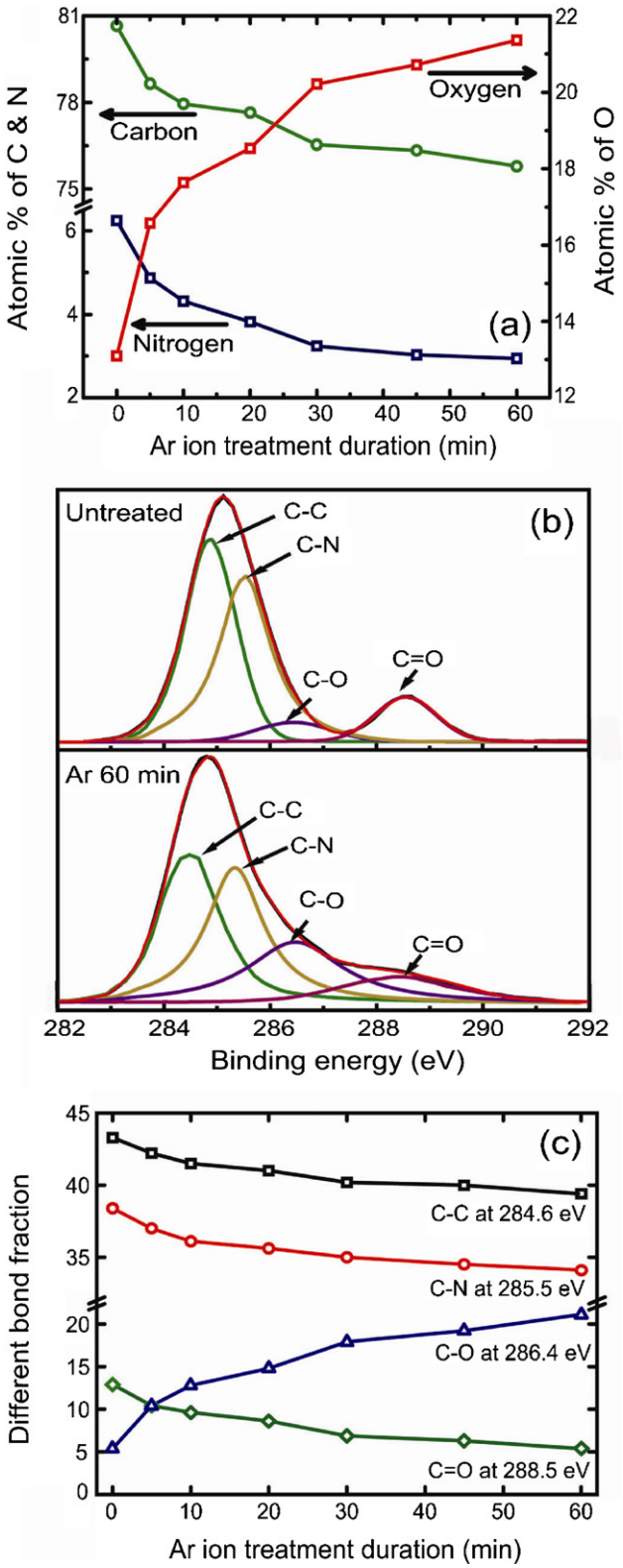

Fig. 3. (a) The variations in the atomic fractions of C, N and O on the PI surface from XPS with respect to the Ar ion beam treatment duration, (b) deconvolution of the C1s peak for the untreated and 60 min Ar ion treated PI and (c) the variations in the bond fraction with respect to the Ar ion beam treatment duration.

the variations in the binding components of the C—C, C—N, C—O, and C=O bonds on the PI surface after the Ar ion beam irradiation. These variations were obtained from the integral intensities of the peaks of each chemical bond in Fig. 3(b). The results in Fig. 3(c) were consistent with Fig. 3(a). As the Ar ion treatment duration increased, the C—C, C—N and C=O bonds decreased from 43.2 to 39.4%, 38.4 to 34.1% and 12.9 to 5.4%, respectively because the C=O and C—N bonds were broken. However, the increase in the components of the C—O bonds from 5.4 to 21.1% was attributed to the rearrangement of the carbon atoms through the formation of the C—O—C, or C—O—N bonds [11]. In general, scissioning and cross-linking occur during the irradiation of PI, and these processes depend upon the type of radiation, the dose rate and the environment such, as ion beam or plasma. Either cross-linking or scissioning can dominate the affected PI layer after ion irradiation [11,21]. XPS as well as the FT-IR analysis revealed that the chain scissioning in PI occurred during the Ar ion beam treatment, which induced the hole and 3D porous nanopattern structures.

3.4. Mechanical properties

Fig. 4(a) shows the variations in the hardness and the elastic modulus of the Ar ion beam treated PI with respect to the treatment duration for a 250 μN load. The hardness and the elastic modulus of Ar ion beam treated PI increased from 1.17 to 1.62 GPa and 4.06 to 5.41 GPa, respectively, with increasing treatment duration. The range that was estimated for the hardness and the elastic modulus of the Ar ion beam treated PI was comparable to the MeV light ions (such as C, H and He) and the Si ions irradiated PI, even though these values depended on the type of radiation, dose rate

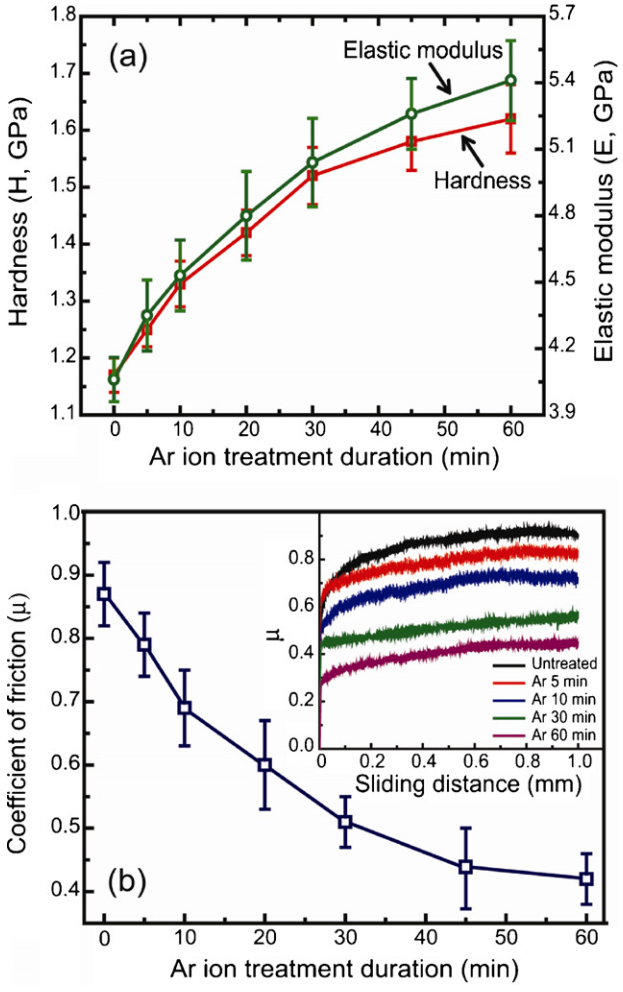

Fig. 4. (a) The changes in the hardness and the elastic modulus of PI that was treated using an Ar ion beam for different treatment durations and (b) the variations in the coefficient of friction with respect to the Ar ion treatment duration. The inset shows the variations in the coefficient of friction with respect to the sliding distance.

and environment, such as ion beam or plasma [10,22,23]. Generally the hardness and the elastic modulus of a polymer increase through a cross-linking phenomena that is induced by ion beam irradiation [10,16,23]. Shah et al. observed the chain scissioning phenomena for PI that was irradiated by 3 MeV protons, and the hardness increased as the fluence increased [24]. The surface hardness and the elastic modulus of the PI surfaces rapidly increased for Ar ion beam treatment durations of up to 30 min and then slowly increased slowly up to 60 min. These results were consistent with the morphological evolution of the holes and the 3D morphology before the treatment duration reached 30 min and the 3D porous nanostructure for treatment durations above 30 min, respectively, in Fig. 1. Generally, the surface nanostructure of the polymer reduces the hardness as well as the elastic modulus [13,16], but the analysis showed that the chemical composition changed because the Ar ion beam treatment played a dominant role in the surface strength or hardness of PI.

Fig. 4(b) shows that the coefficient of friction (μ) for PI decreased with increasing Ar ion beam treatment duration, and the inset shows the changes in the coefficient of friction with respect to the sliding distance. The decreased friction might be due to the increased hardness and the surface nanostructure evolution during the Ar ion beam treatment [22,25]. The results in Fig. 4(b) suggested that the nano-structures evolved after the Ar ion beam treatment, which reduced the contact area as the glass ball slid over the Ar ion beam treated PI surface (see Fig. 1), reducing the coefficient of friction. Also, the coefficient of friction decreased because of the lubricating effects of the graphite-like and carbon-rich amorphous structures that formed on the surface of the polymer during the ion beam irradiation process [17,25].

4. Conclusions

The evolution of the 3D porous nanostructures with a mean diameter of ~90 nm and the mechanical properties of the PI surface were studied using an Ar ion beam treatment for 5–60 min. The chemical composition and the binding energy were analyzed using the FT-IR spectra and the XPS spectra, which revealed that the scissioning of the various bonds in the polymer chain increased with increasing Ar ion treatment duration. The hardness and the elastics modulus of the PI increased from 1.17 to 1.62 GPa and 4.06 to 5.41 GPa, respectively, as the Ar ion beam treatment duration increased because of the changes in the chemical composition during the Ar ion beam treatment. The tribo measurements showed that the coefficient of friction decreased with increasing Ar ion beam treatment duration.

Acknowledgments

This work was supported in part by a grant 2E22200 from the KIST project (KRL), of CNMT under the 21st Century Frontier R&D Programs from MEST (2010K000298), from the KME as Eco-innovation program (Environmental Research Laboratory) (414-111-011 MWM) and in part by a financial support program from Hansung University in 2010 (JIY).

References

[1] M.K. Ghosh, K.L. Mittal (Eds.), Polyimides: Fundamentals and Applications, Marcel Dekker, New York, USA, 1996.
[2] C.C. Wu, S.L.C. Hsu, I.L. Lo, J. Nanosci. Nanotechnol. 10 (2010) 6446.
[3] M.C. Choi, Y. Kim, C.S. Ha, Prog. Polym. Sci. 33 (2008) 581.
[4] I. Ghosh, J. Konar, A.K. Bhowmick, J. Adhes. Sci. Technol. 11 (1997) 877.
[5] T. Ogawa, S. Baba, Y. Fujii, J. Appl. Polym. Sci. 100 (2006) 3403.
[6] A. Baba, K. Higa, T. Asano, Jpn. J. Appl. Phys. 38 (1999) L261.
[7] H. Shimamura, T. Nakamura, Polym. Degrad. Stab. 94 (2009) 1389.
[8] M.H. Kim, K.W. Lee, Met. Mater. Int. 12 (2006) 425.
[9] M.-W. Moon, J.H. Han, A. Vaziri, E.K. Her, K.H. Oh, K.-R. Lee, J.W. Hutchinson, Nanotechnology 20 (2009) 115301.
[10] S.O. Kucheyev, T.E. Felter, M. Anthamatten, J.E. Bradby, Appl. Phys. Lett. 85 (2004) 733.
[11] J.W. Shin, J.P. Jeun, P.H. Kang, Macromol. Res. 18 (2010) 227.
[12] W. Ensinger, Surf. Coat. Technol. 201 (2007) 8442.
[13] S.F. Ahmed, G.H. Rho, J.Y. Lee, S.J. Kim, H.Y. Kim, Y.J. Jang, M.-W. Moon, K.-R. Lee, Surf. Coat. Technol. 205 (2010) L104.
[14] V. Hnatowicz, V. Perina, A. Mackova, V. Svorcik, V. Rybka, D. Fink, J. Heitz, Nucl. Instr. Meth. Phys. Res. B 175 (2007) 437.
[15] J.F. Ziegler, J. Appl. Phys. 85 (1999) 1249.
[16] S.F. Ahmed, J.W. Yi, M.-W. Moon, Y.J. Jang, B.H. Park, S.H. Lee, K.-R. Lee, Plasma Proc. Polym. 6 (2009) 860.
[17] S.F. Ahmed, M.-W. Moon, C. Kim, Y.-J. Jang, S. Han, J.Y. Choi, W.W. Park, K.-R. Lee, Appl. Phys. Lett. 97 (2010) 081908.
[18] M.-W. Moon, S.H. Lee, J.Y. Sun, K.H. Oh, A. Vaziri, J.W. Hutchinson, Proc. Natl. Acad. Sci. U.S.A. 104 (2007) 1130.
[19] D. Fink, F. Hosoi, H. Omichi, T. Sasuga, L. Amaral, Rad. Eff. Def. Solids 132 (1994) 313.
[20] A.M. Ektessabi, S. Hakamata, Thin Solid Films 377–378 (2000) 621.
[21] R. Mishra, S.P. Tripathy, K.K. Dwivedi, D.T. Khathing, S. Ghosh, M. Muller, D. Fink, Rad. Meas. 36 (2003) 621.
[22] T. Chen, S. Yao, K. Wang, H. Wang, Nucl. Instr. Meth. Phys. Res. B 266 (2008) 3091.
[23] H. Dong, T. Bell, Surf. Coat. Technol. 111 (1999) 29.
[24] N. Shah, N.L. Singh, C.F. Desai, K.P. Singh, Rad. Meas. 36 (2003) 699.
[25] J.T. Kim, J.K. Park, D.C. Lee, Polym. Int. 51 (2002) 1063.